Burden of Dilated Perivascular Spaces, an Emerging Marker of Cerebral Small Vessel Disease, Is Highly Heritable

Marie-Gabrielle Duperron, MS; Christophe Tzourio, MD, PhD; Muralidharan Sargurupremraj, PhD; Bernard Mazoyer, MD, PhD; Aïcha Soumaré, PhD; Sabrina Schilling, PhD; Philippe Amouyel, MD, PhD; Ganesh Chauhan, PhD; Yi-Cheng Zhu, MD, PhD; Stéphanie Debette, MD, PhD

Background and Purpose—The genetic contribution to dilated perivascular space (dPVS) burden—an emerging MRI marker of cerebral small vessel disease—is unknown. We measured the heritability of dPVS burden and its shared heritability with other MRI markers of cerebral small vessel disease.

Methods—The study sample comprised 1597 participants from the population-based Three City (3C) Dijon Study, with brain MRI and genome-wide genotyping (mean age, 72.8±4.1 years; 61% women). dPVS burden and lacunar brain infarcts were rated on a semiquantitative scale, whereas an automated algorithm generated white matter hyperintensity volume (WMHV). We estimated dPVS burden heritability and shared heritability with WMHV and lacunar brain infarcts using the genome-wide complex trait analysis tool, on unrelated participants, adjusting for age, sex, intracranial volume, and principal components of population stratification.

Results—dPVS burden was significantly correlated with WMHV and lacunar brain infarcts, the strongest correlation being found between WMHV and dPVS in basal ganglia. Heritability estimates were h^2=0.59±0.24 (*P*=0.007) for dPVS burden, h^2=0.54±0.24 (*P*=0.010) for WMHV, and h^2=0.48±0.81 (*P*=0.278) for lacunar brain infarcts. We found a nonsignificant trend toward shared heritability between dPVS and WMHV (r_g=0.41±0.28; *P*=0.096), which seemed driven by dPVS in basal ganglia (r_g=0.72±0.61; *P*=0.126) and not dPVS in white matter (r_g=−0.10±0.36; *P*=0.393). A genetic risk score for WMHV based on published loci was associated with increased dPVS burden in basal ganglia (*P*=0.031).

Conclusions—We provide evidence for important genetic contribution to dPVS burden in older community-dwelling people, some of which may be shared with WMHV. Differential heritability patterns for dPVS in white matter and basal ganglia suggest at least partly distinct underlying biological processes. **(*Stroke*. 2018;49:282-287. DOI: 10.1161/STROKEAHA.117.019309.)**

Key Words: brain ■ cerebral small vessel diseases ■ humans ■ leukoaraiosis ■ magnetic resonance imaging

Perivascular spaces (PVS), also called Virchow–Robin spaces, are normal physiological structures filled with cerebrospinal MRI signal-like fluid and coated by pial cells, surrounding the wall of arteries, arterioles, veins, and venules as they penetrate into the brain parenchyma. PVS belong to the glymphatic system and are involved in waste clearance, energy substrate delivery, and blood flow regulation.[1,2] Under certain circumstances, such as increasing age and cerebral small vessel disease (cSVD), PVS can dilate (dilated perivascular space [dPVS]) and become detectable on brain MRI.[3–7] Mechanisms underlying this dilation, possibly reflecting reduced glymphatic clearance, are speculative.[1] dPVS were shown to be strongly correlated with other MRI markers of cSVD, such as white matter hyperintensity volume (WMHV), lacunar brain infarcts (LIs), and cerebral microbleeds.[3–6,8] We previously showed that high grades of dPVS in basal ganglia (BG) or white matter (WM) are associated with increased risk of incident dementia, independently of other MRI markers of cSVD, in older community persons.[9]

Determinants of dPVS are poorly understood. The main known risk factors are age and hypertension, the latter being more strongly associated with dPVS in BG. Identifying genetic determinants of dPVS may provide important clues on underlying molecular mechanisms and on cSVD and

Received September 5, 2017; final revision received November 21, 2017; accepted November 29, 2017.

From the Inserm, Bordeaux Population Health Research Center (M-G.D., C.T., M.S., A.S., S.S., G. C., S.D.) and Institut des Maladies Neurodégénératives, CNRS-CEA UMR 5293 (B.M.), University of Bordeaux, France; Pole de santé publique (C.T.) and Department of Neurology (S.D.), Centre Hospitalier Universitaire de Bordeaux, France; Inserm U1167, Lille, France (P.A.); Department of Epidemiology and Public Health, Pasteur Institute of Lille, France (P.A.); Department of Public Health, Lille University Hospital, France (P.A.); Centre for Brain Research, Indian Institute of Science, Bangalore, India (G.C.); and Department of Neurology, Pekin Union Medical College Hospital, Beijing, China (Y.-C.Z.).

The online-only Data Supplement is available with this article at http://stroke.ahajournals.org/lookup/suppl/doi:10.1161/STROKEAHA.117.019309/-/DC1.

Correspondence to Stéphanie Debette, MD, PhD, Inserm U1219, Bordeaux Population Health Research Center, University of Bordeaux, 146 Rue Léo Saignat, 33076 Bordeaux, France. E-mail stephanie.debette@u-bordeaux.fr

dementia pathophysiology. We sought to examine the genetic contribution to dPVS burden by measuring their heritability and shared heritability with other MRI markers of cSVD in the population-based Three City (3C) Dijon Study.

Methods

The data that support the findings of this study are available from the corresponding author on reasonable request.

Study Population

The 3C-Dijon Study is a community-based cohort study comprising 4931 noninstitutionalized participants aged ≥65 years randomly selected from the electoral rolls of the city of Dijon between 1999 and 2001.[10] Participants aged <80 years and enrolled between June 1999 and September 2000 (n=2763) were invited to undergo a brain MRI. Although 2285 participants (82.7%) agreed to participate because of financial limitations, MRI scans were performed in 1924 participants only. Among these, 1683 had also undergone genome-wide genotyping. After exclusion of individuals with brain tumors (n=8), stroke (n=71), or dementia (n=7) at baseline, the remaining sample comprised 1597 participants. Visual assessment and quantification was available in 1559 participants for dPVS and 1562 participants for LI (35 individuals with non-lacunar brain infarcts were excluded); and 1495 participants had automated quantitative WMHV measurements. The study protocol was approved by the ethical committee of the University Hospital of Kremlin-Bicêtre. All participants provided written informed consent.

Genotyping

DNA samples of 3C-Dijon participants were genotyped with Illumina Human610Iquad BeadChips at the Centre National de Génotypage, Evry, France.

Genotyping was performed on 4263 participants, of whom 186 were excluded after quality control (Methods in the online-only Data Supplement), leaving a total of 4077 participants. The first 20 principal components (PCs) for the 3C-Dijon sample were generated using EIGENSOFT and used to correct for population ancestry stratification (Methods in the online-only Data Supplement). Genotypes were imputed to the 1000 Genomes phase I version 3 reference panel (all ethnicities) using MaCH 1.0, after applying standard quality control procedures (Methods in the online-only Data Supplement). In total, 11 572 501 single-nucleotide polymorphisms (SNPs) were available for analysis after quality control.

MRI Acquisition

MRI acquisition was performed on a 1.5-Tesla Magnetom scanner (Siemens). A 3-dimensional high-resolution T1-, T2-, and PD- (proton density) weighted brain volumes were acquired (Methods in the online-only Data Supplement).

Rating of dPVS

dPVS were evaluated by an experienced reader (Y.-C.Z.) and quantified on a semiquantitative scale. They were defined as cerebrospinal fluid-like signal lesions (hypointense on T1 and hyperintense on T2) of round, ovoid, or linear shape with a maximum diameter <3 mm, having smooth delineated contours, and located in areas supplied by perforating arteries. Lesions fulfilling the same criteria except for a diameter ≥3 mm were carefully examined in the 3 planes (shape, signal intensity) to differentiate them from LI and white matter hyperintensity (WMH). Only lesions with a typical vascular shape and those that followed the orientation of perforating vessels were considered dPVS.[3] In BG and WM, which are the locations with the highest density of dPVS, the slice containing the greatest number of dPVS was used for the rating.[3]

In BG, dPVS were rated using a 4-grade score: grade 1 for <5 dPVS, grade 2 for 5 to 10 dPVS, grade 3 for >10 dPVS but still numerable, and grade 4 for innumerable dPVS resulting in a cribriform change in BG (Figure). In the WM, dPVS were also rated using a 4-grade score: grade 1 for <10 dPVS in the total WM, grade 2 for >10 dPVS in the total WM and <10 in the slice containing the greatest number of dPVS, grade 3 for 10 to 20 dPVS in the slice containing the greatest number of dPVS, and grade 4 for >20 dPVS in the slice containing the greatest number of dPVS (Figure).[3] In the hippocampus and brain stem, dPVS were dichotomized as presence of ≥1 dPVS versus none. A global dPVS burden variable was constructed by summing up dPVS grades in BG and WM and adding 1 point for the presence of ≥1 dPVS in the hippocampus and 1 point for the presence of ≥1 dPVS in the brain stem. Because of the small number of participants in the highest categories, these were combined (global score ≥8). The global variable was normally distributed on visual inspection (Methods in the online-only Data Supplement).

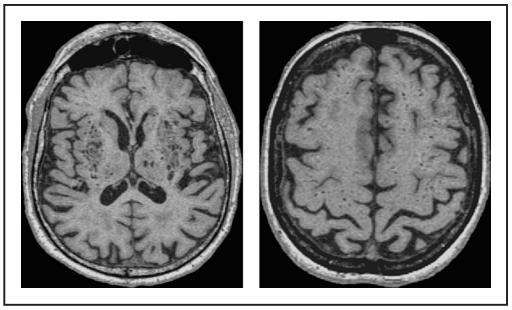

Figure. Grade 4 of dilated perivascular space burden in basal ganglia (**left**) and in white matter (**right**)[3] (axial T1-weighted images, 3C-Dijon Study).

Other MRI Measurements

An automated and validated procedure was used to localize and measure WMHV.[11] Two subgroups of WMH were defined: periventricular WMH (pvWMH) when the distance to the ventricular system was <10 mm and deep WMH otherwise. LIs were evaluated visually by the same rater (Y.-C.Z.) as dPVS and were defined as focal lesions with the same signal characteristics as cerebrospinal fluid on all sequences and with a diameter of 3 to 15 mm.[3] They were differentiated from dPVS as described above. The gray matter, WM, and cerebrospinal fluid volumes were estimated using voxel-based morphometry; intracranial volume (ICV) was calculated by summing these 3 volumes.[12]

Statistical Analysis

Global dPVS burden was analyzed as a continuous variable, given its normal distribution, whereas dPVS subtypes (WM and BG) were studied as dichotomized variables (grade 3–4 versus grade 1–2). Because WMHV had a skewed distribution, we used natural log-transformed values (Ln[WMHV+1.0]), as in previous analyses.[13,14] Phenotypic correlation between MRI markers of cSVD was calculated based on Spearman correlation using SAS software, version 9.3 (SAS Institute, Inc, Cary, NC).

To estimate heritability for dPVS, WMHV, and LI, we used genome-wide complex trait analysis (GCTA v1.26.0). This corresponds to estimating the proportion of phenotypic variance of MRI markers of cSVD explained by all common SNPs available genome wide, using a linear mixed model analysis (Methods in the online-only Data Supplement).[15] We then assessed the proportion of shared heritability between dPVS burden and WMHV using SNP-derived genomic relationships and genomic relatedness-based restricted maximum likelihood (bivariate GREML method).[16] Using this method, implemented in the genome-wide complex trait analysis software, we could estimate the genetic correlation between dPVS burden and WMHV (overall and by main subtypes, Methods in the online-only Data Supplement). Estimation of genetic correlation with LI was not possible (models did not converge or yield aberrant values). All analyses for heritability and shared heritability were performed on unrelated individuals, after removing randomly 1 individual of each pair with estimated relatedness >0.125 (genetic relatedness matrix >0.125). Analyses of dPVS burden and WMHV were adjusted for

ICV, to account for differences in head size, age, sex, and 20 PCs, as recommended by the software.[15]

We tested for association of a genetic risk score combining known independent genetic risk variants for WMHV (rs7214628, rs7894407, rs78857879, rs2984613, and rs11679640)[14] with dPVS burden using linear regression (dPVS global) or logistic regression (dPVS in WM and in BG), adjusting for age, sex, the first 4 PCs, and ICV. The genetic risk score was constructed by summing up the number of WMHV risk alleles across all independent WMHV risk loci (r^2<0.010 between SNPs). This score was unweighted because the WMHV genome-wide association study from which risk loci were derived was performed using *z* score-based meta-analysis, which does not yield any effect estimate.

Results

Study Population

Characteristics of the study population are shown in Table 1. The mean age was 72.8±4.1 years, and 60.9% of participants were women. All participants had some dPVS. The prevalence of participants with dPVS burden of grade 3 to 4 was 11.4% (95% confidence interval [CI], 9.8%–13.0%) in BG, and 22.8% (CI, 20.7%–24.9%) in WM; 44.7% (CI, 42.2%–47.2%) of participants had at least 1 dPVS in the hippocampus, and 66.5% (CI, 64.1%–68.8%) had at least 1 dPVS in the brain stem. The prevalence of LI was 7.5% (CI, 6.2%–8.8%). Mean WMHV was 5.49±4.73 cm^3 (4.02±4.00 cm^3 for pvWMHV and 1.47±1.17 cm^3 for deep WMHV). Participants included in the analysis had on average fewer vascular risk factors and were younger than 3C Dijon participants aged <80 years at inclusion who were not included (Table I in the online-only Data Supplement).

Table 1. Characteristics of Study Participants (3C-Dijon Study, n=1562 With Brain MRI and Cerebral Small Vessel Disease Assessment)

Characteristics	
Age at MRI, y, mean±SD	72.8±4.1
Women, n (%)	951 (60.9)
Systolic blood pressure, mm Hg	148.8±22.7
Diastolic blood pressure, mm Hg	84.9±11.5
Pulse pressure, mm Hg	63.9±17.1
Hypertension status*	1197 (76.6)
Type II diabetes mellitus†	130 (8.34)
Current smoker	95 (6.1)
History of cardiovascular disease‡	64 (4.1)
Body mass index, kg/m^2	25.5±3.85
Hypercholesterolemia§	876 (56.2)
Total cholesterol, mmol/L	5.8±0.9
Low-density lipoprotein, mmol/L	3.6±0.8
Triglycerides, mmol/L	1.2±0.6
High-density lipoprotein, mmol/L	1.6±0.4
Educational level >baccalaureate‖	557 (35.7)

MRI indicates magnetic resonance imaging.

*Systolic blood pressure ≥140 mm Hg or diastolic blood pressure ≥90 mm Hg or antihypertensive drugs.

†Blood glucose ≥7 mmol/L±antidiabetic drugs.

‡Include myocardial infarction, arteritis, and cardiac and vascular surgery (patients with stroke excluded).

§Cholesterolemia ≥6.2 mmol/L or lipid-lowering treatment.

‖Final high-school degree in France.

Phenotypic Correlations

There was limited but significant phenotypic correlation (ρ=0.23; *P*<0.0001) between dPVS in BG and dPVS in WM—the 2 main subtypes of dPVS. Phenotypic correlations between dPVS and other MRI markers of cSVD are represented in Table 2: all markers showed some degree of correlation at *P*<0.01 (ρ ranging between 0.08 and 0.33). The highest phenotypic correlation coefficient (ρ=0.33; *P*<0.0001) was observed between dPVS in BG and total WMHV or pvWMHV. The correlation between dPVS (global) and LI was lower, at 0.18 (*P*<0.0001; Table 2).

Heritability Analysis of dPVS and Other MRI Markers of cSVD

The age, sex, ICV, and 20 PC-adjusted heritability for dPVS (global) was estimated at 59% (*P*=0.007) and was highest and significant in the WM, estimated at 79% (*P*=0.042), compared with BG (Table 3). Heritability for presence of dPVS in hippocampus and brain stem was low (<4%) and nonsignificant. In a secondary analysis, taking the top quartile of dPVS count in hippocampus and brain stem instead of presence versus absence, heritability for dPVS in hippocampus was found to be higher but still nonsignificant (Table II in the online-only Data Supplement). Comparatively, the age, sex, ICV, and 20 PC-adjusted heritability for WMHV was evaluated at 54% (*P*=0.010) and significant for pvWMHV and deep WMHV, whereas the age, sex, and 20 PC-adjusted heritability for LI was lower and nonsignificant (48%; *P*=0.278; Table 3). Of note, heritability estimates of dPVS and other MRI markers of cSVD were substantially unchanged after adjusting for hypertension and diabetes mellitus—the 2 main known risk factors for cSVD (Tables III and IV in the online-only Data Supplement).

Shared Heritability of dPVS With Other MRI Markers of cSVD

We found a shared heritability estimate of dPVS (global) with WMHV at 41% (*P*=0.096); shared heritability with

Table 2. Phenotypic Correlations of dPVS Burden With Other Magnetic Resonance Imaging Markers of Cerebral Small Vessel Disease

	ρ With WMHV (n=1490)	ρ With dWMHV (n=1490)	ρ With pvWMHV (n=1490)	ρ With LI (n=1534)
dPVS (global)	0.27*	0.29*	0.22*	0.18*
dPVS (WM)	0.15*	0.26*	0.08†	0.12*
dPVS (BG)	0.33*	0.22*	0.33*	0.23*

Numbers in the cells correspond to Spearman correlation coefficient (ρ). BG indicates basal ganglia; dPVS, dilated perivascular spaces; dWMHV, deep white matter hyperintensity volume; LI, lacunar brain infarcts; pvWMHV, periventricular white matter hyperintensity volume; WM, white matter; and WMHV, white matter hyperintensity volume.

*P<0.0001.

†P<0.01.

Table 3. Heritability of Magnetic Resonance Imaging Markers of Cerebral Small Vessel Disease Estimated Using Genome-Wide Complex Trait Analysis

	h^2 (SD)	*P* Value	n*
dPVS (global)	0.59 (0.24)	0.007	1482
dPVS (WM)	0.79 (0.46)	0.042	1482
dPVS (BG)	0.40 (0.65)	0.270	1482
dPVS (HIP)	0.04 (0.39)	0.462	1482
dPVS (BS)	0.003 (0.39)	0.497	1482
WMHV	0.54 (0.24)	0.010	1482
dWMHV	0.64 (0.24)	0.004	1482
pvWMHV	0.52 (0.24)	0.013	1482
LI	0.48 (0.81)	0.278	1549

Analyses were adjusted for age, sex, first 20 principal components of population stratification (dPVS, WMHV and LI), and intracranial volume (only for dPVS and WMHV). BG indicates basal ganglia; BS, brain stem; dPVS, dilated perivascular spaces; dWMHV, deep white matter hyperintensity; h2, proportion of phenotypic variance explained by genome-wide single-nucleotide polymorphisms; HIP, hippocampus; LI, lacunar brain infarcts; pvWMHV, periventricular white matter hyperintensity; WM, white matter; and WMHV, white matter hyperintensity volume.

*Unrelated individuals up to the third degree.

deep WMHV (38%; *P*=0.095) was in the same range as with pvWMHV (40%; *P*=0.100). Shared heritability between dPVS and WMHV was driven by dPVS in BG (72%; *P*=0.126) and not dPVS in WM (Table 4).

Association of Known Risk Variants for WMHV With dPVS Burden

We found a nominally significant association of a genetic risk score combining all published independent WMHV risk variants with dPVS in BG (*P*=0.031), with WMHV risk alleles in aggregate being associated with increased risk of high dPVS grades in BG (Table 5). Of note, this association was not driven by a single risk variant for WMHV (*P*>0.09 for individual SNP–dPVS associations; Table V in the online-only Data Supplement).

Discussion

In a large population-based study of >1500 stroke- and dementia-free older unrelated persons, we found high heritability estimates, derived from genome-wide genotypes, for dPVS burden, in the same range as heritability estimates for WMHV, whereas heritability of LI was lower. Some of the estimated heritability for dPVS and WMHV appears to be shared. We found highest genetic correlation between dPVS in BG and WMHV, consistent with the high phenotypic correlation observed between WMHV and dPVS in this location. We also found a nominally significant association between a genetic risk score combining known genetic risk variants for WMHV and dPVS in BG.

Heritability of dPVS has not been described before to our knowledge. For WMHV and LI, our results are consistent with estimates from family-based studies, showing moderate-to-high heritability for WMH burden (49%–80%)[17–21] and lower heritability for LI (29%).[21] Of note, heritability estimates from family-based studies are always larger than SNP-derived heritability estimates because they represent only the narrow-sense heritability.[22]

The stronger genetic correlation of WMHV with dPVS burden in BG than in WM strengthens the hypothesis of at least partly distinct processes underlying dPVS in these 2 locations.[9] We previously described that the severity of dPVS in both in BG and WM does not necessarily coincide. Indeed, among individuals with grade 4 of dPVS in WM, only 23% also had a grade 3 or 4 in BG, and among individuals with grade 4 of dPVS in BG, 42% also had a grade 3 or 4 in WM.[3] We and others have also shown that vascular risk factor profiles vary according to the dPVS location.[3,23] This is further corroborated by the present findings, showing a stronger phenotypic correlation and shared genetic variation between WMHV and dPVS in BG compared with dPVS in WM. Interestingly, only severity of dPVS in BG was associated with a higher rate of cognitive decline in older community persons from the 3C-Dijon Study[9] and with worse processing speed performance in a cohort of patients with cSVD or at high risk of cSVD.[24] Interleukin-6 levels were associated with higher severity of dPVS in BG but not in WM.[25] Hence, there seems to be converging evidence that dPVS may have at least partly distinct underlying risk factors, including genetic, and clinical consequences depending on their location.

The mechanisms underlying PVS dilation are speculative. One of the hypotheses is a reduction of cerebrospinal fluid production with aging, leading to a decrease in glymphatic clearance and an accumulation of toxic proteins.[26–28] In parallel, the arterial wall stiffening occurring with aging or disease may lead to a reduction in arterial pulsatility, facilitating dilation of PVS.[28,29] Astrocytic hypertrophy and loss of perivascular aquaporin-4 polarization, leading to dysregulation of astroglial water transport, as well as blood–brain barrier dysfunction might also be involved.[30–33] Most hypothetical

Table 4. Shared Heritability Between dPVS and WMHV (n=1482)

	r_g (SD) With WMHV	*P* Value	r_g (SD) With dWMHV	*P* Value	r_g (SD) With pvWMHV	*P* Value
dPVS (global)	0.41 (0.28)	0.096	0.38 (0.25)	0.095	0.40 (0.30)	0.100
dPVS (WM)	–0.10 (0.36)	0.393	0.09 (0.33)	0.401	–0.10 (0.37)	0.394
dPVS (BG)	0.72 (0.61)	0.126	0.60 (0.63)	0.155	0.68 (0.60)	0.144

Analyses were adjusted for age, sex, first 20 principal components for population stratification, and intracranial volume. BG indicates basal ganglia; dPVS, dilated perivascular spaces; dWMHV, deep white matter hyperintensity volume; pvWMHV, periventricular white matter hyperintensity volume; rg, genetic correlation between genetic effects across traits; WM, white matter; and WMHV, white matter hyperintensity volume.

Table 5. Association of a Genetic Risk Score for WMHV With dPVS Burden (n=1494)

	Genetic Risk Score for WMHV	
	β (SD) or OR (95% CI)	*P* Value
dPVS (global)*	0.01 (0.03)	0.783
dPVS (WM)†	0.98 (0.89–1.08)	0.704
dPVS (BG)†	1.15 (1.01–1.30)	0.031

Analyses were adjusted for age, sex, first 4 principal components of population stratification, and intracranial volume. BG indicates basal ganglia; CI, confidence interval; dPVS, dilated perivascular spaces; OR, odds ratio; WM, white matter; and WMHV, white matter hyperintensity volume.

*Linear regression.

†Logistic regression.

pathophysiological pathways for dPVS are derived from animal models. Exploring the genetic determinants of dPVS using an unbiased genome-wide approach may provide additional insight into the biological pathways underlying dPVS in humans, potentially providing further evidence for one or more of the aforementioned hypotheses or suggesting novel previously unsuspected mechanisms. The high SNP-derived heritability estimates for dPVS burden suggest that searching for genetic determinants of dPVS could indeed be an efficient approach. Although the genetic correlation between WMHV and dPVS was relatively high, a substantial proportion of genetic contribution to dPVS burden appears not to be shared with other MRI markers of cSVD, warranting efforts to decipher specifically the genetics of dPVS burden. Increasing the number of participants and harmonizing dPVS measurements across existing studies,[34] as well as taking into account confounding and effect modification by environmental risk factors, especially hypertension, will be important for future endeavors.

Strengths of our study include a large sample size in a population-based setting with careful rating of dPVS by the same experienced reader using whole-brain MR images with precise assessment of dPVS shape on 3-dimensional millimetric T1 images and differentiation from WMH and LI using careful examination in the 3 planes and exploration of T2 and proton density sequences. Efforts to develop automated and quantitative assessment of dPVS burden are under way but not yet available for large-scale use. Stringent quality control criteria with strict removal of related individuals and adjustment for the 20 first PCs were used. Because MRI markers of small vessel disease are strongly correlated with age,[3,35] we cannot exclude residual confounding by age, although our age range at the time of MRI was relatively limited and restricted to older individuals (65–80 years). Future studies on larger samples enabling analyses stratified on narrower age ranges and also including younger age groups in whom cSVD burden may be more heritable could be of interest. Caution is warranted when interpreting the absolute values of heritability and shared heritability, given the relatively limited sample size, especially for the shared heritability analyses that do not reach statistical significance, and should, therefore, be considered as exploratory. Comparison with future similar analyses in independent samples will be needed to obtain more precise estimates.

Conclusions

The present study provides preliminary evidence for an important genetic contribution to dPVS burden in older community persons, suggesting that searching for genetic risk factors of dPVS may be an efficient way to explore the biological mechanisms underlying dPVS and to identify individuals at high risk of cSVD and its consequences. Further studies are also needed to better explore the clinical significance and importance of dPVS, with possible implications for prevention of both cerebrovascular and neurodegenerative disease.

Acknowledgments

We thank the participants of the 3C Study, for their important contributions.

Sources of Funding

The 3C Study is conducted under a partnership agreement among the Institut National de la Santé et de la Recherche Médicale (INSERM), the University of Bordeaux, and Sanofi-Aventis. The Fondation pour la Recherche Médicale funded the preparation and initiation of the study. The 3C Study is also supported by the Caisse Nationale Maladie des Travailleurs Salariés, Direction Générale de la Santé, Mutuelle Générale de l'Education Nationale, Institut de la Longévité, Conseils Régionaux of Aquitaine and Bourgogne, Fondation de France, and Ministry of Research–INSERM Programme Cohortes et collections de données biologiques. This work was supported by the National Foundation for Alzheimer's Disease and Related Disorders, INSERM, the Fédération pour la Recherche sur le Cerveau, Rotary, Lille Génopôle, the Institut Pasteur de Lille, the Centre National de Génotypage, the University of Lille, the Centre Hospitalier Universitaire de Lille, and the Laboratoire d'excellence Development of Innovative Strategies for a Transdisciplinary Approach to Alzheimer's disease. Drs Debette and Tzourio are recipients of a grant from the French National Research Agency, a grant from the Fondation Leducq, and from the Joint Programme for Neurodegenerative Disease Research. Dr Debette is recipient of a grant from the European Research Council.

Disclosures

None.

References

1. Jessen NA, Munk AS, Lundgaard I, Nedergaard M. The glymphatic system: a beginner's guide. *Neurochem Res*. 2015;40:2583–2599. doi: 10.1007/s11064-015-1581-6.
2. Marín-Padilla M, Knopman DS. Developmental aspects of the intracerebral microvasculature and perivascular spaces: insights into brain response to late-life diseases. *J Neuropathol Exp Neurol*. 2011;70:1060–1069. doi: 10.1097/NEN.0b013e31823ac627.
3. Zhu YC, Tzourio C, Soumaré A, Mazoyer B, Dufouil C, Chabriat H. Severity of dilated Virchow-Robin spaces is associated with age, blood pressure, and MRI markers of small vessel disease: a population-based study. *Stroke*. 2010;41:2483–2490. doi: 10.1161/STROKEAHA.110.591586.
4. Doubal FN, MacLullich AM, Ferguson KJ, Dennis MS, Wardlaw JM. Enlarged perivascular spaces on MRI are a feature of cerebral small vessel disease. *Stroke*. 2010;41:450–454. doi: 10.1161/STROKEAHA.109.564914.
5. Rouhl RP, van Oostenbrugge RJ, Knottnerus IL, Staals JE, Lodder J. Virchow-Robin spaces relate to cerebral small vessel disease severity. *J Neurol*. 2008;255:692–696. doi: 10.1007/s00415-008-0777-y.
6. Potter GM, Doubal FN, Jackson CA, Chappell FM, Sudlow CL, Dennis MS, et al. Enlarged perivascular spaces and cerebral small vessel disease. *Int J Stroke*. 2015;10:376–381. doi: 10.1111/ijs.12054.
7. Kwee RM, Kwee TC. Virchow-Robin spaces at MR imaging. *Radiographics*. 2007;27:1071–1086. doi: 10.1148/rg.274065722.
8. Yakushiji Y, Charidimou A, Hara M, Noguchi T, Nishihara M, Eriguchi M, et al. Topography and associations of perivascular spaces in healthy

adults: the Kashima scan study. *Neurology*. 2014;83:2116–2123. doi: 10.1212/WNL.0000000000001054.
9. Zhu YC, Dufouil C, Soumaré A, Mazoyer B, Chabriat H, Tzourio C. High degree of dilated Virchow-Robin spaces on MRI is associated with increased risk of dementia. *J Alzheimers Dis*. 2010;22:663–672. doi: 10.3233/JAD-2010-100378.
10. 3C Study Group. Vascular factors and risk of dementia: design of the three-city study and baseline characteristics of the study population. *Neuroepidemiology*. 2003;22:316–325. doi: 10.1159/000072920.
11. Maillard P, Delcroix N, Crivello F, Dufouil C, Gicquel S, Joliot M, et al. An automated procedure for the assessment of white matter hyperintensities by multispectral (T1, T2, PD) MRI and an evaluation of its between-centre reproducibility based on two large community databases. *Neuroradiology*. 2008;50:31–42. doi: 10.1007/s00234-007-0312-3.
12. Debette S, Wolf C, Lambert JC, Crivello F, Soumaré A, Zhu YC, et al. Abdominal obesity and lower gray matter volume: a Mendelian randomization study. *Neurobiol Aging*. 2014;35:378–386. doi: 10.1016/j.neurobiolaging.2013.07.022.
13. Fornage M, Debette S, Bis JC, Schmidt H, Ikram MA, Dufouil C, et al. Genome-wide association studies of cerebral white matter lesion burden: the CHARGE consortium. *Ann Neurol*. 2011;69:928–939. doi: 10.1002/ana.22403.
14. Verhaaren BF, Debette S, Bis JC, Smith JA, Ikram MK, Adams HH, et al. Multiethnic genome-wide association study of cerebral white matter hyperintensities on MRI. *Circ Cardiovasc Genet*. 2015;8:398–409. doi: 10.1161/CIRCGENETICS.114.000858.
15. Yang J, Lee SH, Goddard ME, Visscher PM. GCTA: a tool for genome-wide complex trait analysis. *Am J Hum Genet*. 2011;88:76–82. doi: 10.1016/j.ajhg.2010.11.011.
16. Lee SH, Yang J, Goddard ME, Visscher PM, Wray NR. Estimation of pleiotropy between complex diseases using single-nucleotide polymorphism-derived genomic relationships and restricted maximum likelihood. *Bioinformatics*. 2012;28:2540–2542. doi: 10.1093/bioinformatics/bts474.
17. Atwood LD, Wolf PA, Heard-Costa NL, Massaro JM, Beiser A, D'Agostino RB, et al. Genetic variation in white matter hyperintensity volume in the Framingham Study. *Stroke*. 2004;35:1609–1613. doi: 10.1161/01.STR.0000129643.77045.10.
18. Turner ST, Jack CR, Fornage M, Mosley TH, Boerwinkle E, de Andrade M. Heritability of leukoaraiosis in hypertensive sibships. *Hypertension*. 2004;43:483–487. doi: 10.1161/01.HYP.0000112303.26158.92.
19. Kochunov P, Glahn D, Winkler A, Duggirala R, Olvera RL, Cole S, et al. Analysis of genetic variability and whole genome linkage of whole-brain, subcortical, and ependymal hyperintense white matter volume. *Stroke*. 2009;40:3685–3690. doi: 10.1161/STROKEAHA.109.565390.
20. DeStefano AL, Seshadri S, Beiser A, Atwood LD, Massaro JM, Au R, et al. Bivariate heritability of total and regional brain volumes: the Framingham Study. *Alzheimer Dis Assoc Disord*. 2009;23:218–223. doi: 10.1097/WAD.0b013e31819cadd8.
21. Sachdev PS, Lee T, Wen W, Ames D, Batouli AH, Bowden J, et al; OATS Research Team. The contribution of twins to the study of cognitive ageing and dementia: the Older Australian Twins Study. *Int Rev Psychiatry*. 2013;25:738–747. doi: 10.3109/09540261.2013.870137.
22. Visscher PM, Goddard ME. A general unified framework to assess the sampling variance of heritability estimates using pedigree or marker-based relationships. *Genetics*. 2015;199:223–232. doi: 10.1534/genetics.114.171017.
23. Zhang C, Chen Q, Wang Y, Zhao X, Wang C, Liu L, et al; Chinese IntraCranial AtheroSclerosis (CICAS) Study Group. Risk factors of dilated Virchow-Robin spaces are different in various brain regions. *PLoS One*. 2014;9:e105505. doi: 10.1371/journal.pone.0105505.
24. Huijts M, Duits A, Staals J, Kroon AA, de Leeuw PW, van Oostenbrugge RJ. Basal ganglia enlarged perivascular spaces are linked to cognitive function in patients with cerebral small vessel disease. *Curr Neurovasc Res*. 2014;11:136–141.
25. Satizabal CL, Zhu YC, Dufouil C, Tzourio C. Inflammatory proteins and the severity of dilated Virchow-Robin Spaces in the elderly. *J Alzheimers Dis*. 2013;33:323–328. doi: 10.3233/JAD-2012-120874.
26. Fleischman D, Berdahl JP, Zaydlarova J, Stinnett S, Fautsch MP, Allingham RR. Cerebrospinal fluid pressure decreases with older age. *PLoS One*. 2012;7:e52664. doi: 10.1371/journal.pone.0052664.
27. Chen RL, Kassem NA, Redzic ZB, Chen CP, Segal MB, Preston JE. Age-related changes in choroid plexus and blood-cerebrospinal fluid barrier function in the sheep. *Exp Gerontol*. 2009;44:289–296. doi: 10.1016/j.exger.2008.12.004.
28. Iliff JJ, Wang M, Zeppenfeld DM, Venkataraman A, Plog BA, Liao Y, et al. Cerebral arterial pulsation drives paravascular CSF-interstitial fluid exchange in the murine brain. *J Neurosci*. 2013;33:18190–18199. doi: 10.1523/JNEUROSCI.1592-13.2013.
29. Zieman SJ, Melenovsky V, Kass DA. Mechanisms, pathophysiology, and therapy of arterial stiffness. *Arterioscler Thromb Vasc Biol*. 2005;25:932–943. doi: 10.1161/01.ATV.0000160548.78317.29.
30. Sabbatini M, Barili P, Bronzetti E, Zaccheo D, Amenta F. Age-related changes of glial fibrillary acidic protein immunoreactive astrocytes in the rat cerebellar cortex. *Mech Ageing Dev*. 1999;108:165–172.
31. Kress BT, Iliff JJ, Xia M, Wang M, Wei HS, Zeppenfeld D, et al. Impairment of paravascular clearance pathways in the aging brain. *Ann Neurol*. 2014;76:845–861. doi: 10.1002/ana.24271.
32. Wardlaw JM. Blood-brain barrier and cerebral small vessel disease. *J Neurol Sci*. 2010;299:66–71. doi: 10.1016/j.jns.2010.08.042.
33. Iliff JJ, Wang M, Liao Y, Plogg BA, Peng W, Gundersen GA, et al. A paravascular pathway facilitates CSF flow through the brain parenchyma and the clearance of interstitial solutes, including amyloid β. *Sci Transl Med*. 2012;4:147ra111. doi: 10.1126/scitranslmed.3003748.
34. Adams HH, Hilal S, Schwingenschuh P, Wittfeld K, van der Lee SJ, DeCarli C, et al. A priori collaboration in population imaging: the Uniform Neuro-Imaging of Virchow-Robin Spaces Enlargement consortium. *Alzheimers Dement (Amst)*. 2015;1:513–520. doi: 10.1016/j.dadm.2015.10.004.
35. Debette S, Seshadri S, Beiser A, Au R, Himali JJ, Palumbo C, et al. Midlife vascular risk factor exposure accelerates structural brain aging and cognitive decline. *Neurology*. 2011;77:461–468. doi: 10.1212/WNL.0b013e318227b227.

Burden of Dilated Perivascular Spaces, an Emerging Marker of Cerebral Small Vessel Disease, Is Highly Heritable

Marie-Gabrielle Duperron, Christophe Tzourio, Muralidharan Sargurupremraj, Bernard Mazoyer, Aïcha Soumaré, Sabrina Schilling, Philippe Amouyel, Ganesh Chauhan, Yi-Cheng Zhu and Stéphanie Debette

Stroke. 2018;49:282-287; originally published online January 8, 2018;
doi: 10.1161/STROKEAHA.117.019309
Stroke is published by the American Heart Association, 7272 Greenville Avenue, Dallas, TX 75231

Print ISSN: 0039-2499. Online ISSN: 1524-4628

SUPPLEMENTAL MATERIAL

METHODS

Genotyping quality control and imputation

Genotyping was performed on 4,263 participants, of which 186 were excluded for the following reasons: non-Caucasian ethnicity (n=20), first degree relatives (n=128), call rate <0.95, gender inconsistencies and population stratification outliers (>6 standard deviations from the mean of the corresponding principal component for population stratification (PC), n=38), leaving a total of 4,077 participants.
Genotypes were imputed to the 1000 Genomes phase I version 3 reference panel (all ethnicities) using MaCH 1.0,[1, 2] after applying standard quality control procedures (call rates of <98%, minor allele frequencies <1%, Hardy-Weinberg equilibrium $p<10^{-6}$ and INFO score>0.3).

Principal component (PC) analysis of genetic data

Population stratification – population containing genetically distinct subgroups, with systematic allele frequencies differences due to ancestry differences– may lead to spurious associations and minimize power. To determine a homogenous European ancestry sample, PC analysis was performed based on allele frequencies using EIGENSOFT®.[3] PC analysis was applied to genotype data in order to infer continuous axes of genetic variation. The PC analysis algorithm reduces data dimension to a few principal components describing as much variability as possible. In the present study, analyses were adjusted for the first 20 PCs.

MRI acquisition

The parameters of MRI acquisition were as follows. A high resolution T1-weighted brain volume was acquired using a 3D inversion recovery fast spoiled-gradient echo sequence (3D IR-SPGR; repetition time [TR]=97 ms; echo time [TE]=4 ms; inversion time [TI]=600 ms; coronal acquisition). The axially reoriented 3D volume matrix size was 256×192×256 with a voxel size of 1.0×0.98×0.98 mm^3. T2- and proton density weighted brain volumes were acquired using a 2D fast spin echo sequence with two echo times ([TR]=4400 ms; [TE]1=16 ms; [TE]2=98 ms). T2 and proton density acquisitions consisted of 35 axial slices 3.5 mm thick (0.5 mm between slices spacing), having a 256×256 matrix size and a 0.98×0.98 mm^2 in-plane resolution.

Genome wide complex trait analysis (GCTA) models

Narrow sense (additive) heritability of MRI-phenotypes was performed using GCTA software[4]:

$$h^2 = \frac{\sigma^2_g}{\sigma^2_p}$$

where σ^2_g is the variance explained by all the SNPs and σ^2_p is the phenotypic variance.
All the genotyped and imputed SNPs were treated as random effects and were fitted to a linear mixed model. These estimates are based only on the autosomal SNPs.
Stringent quality control filters were applied to this data set as follows: individuals whose genetic relatedness exceeded 12.5% were excluded from the analysis. Including close relatives would result in the estimate of genetic variance being biased by the phenotypic correlations for these individuals. The removal of close relatives was achieved by using the standardized genotype matrix to create a genetic relationship matrix (GRM) which estimates the genetic relationships between individuals from the SNPs included in the analysis.

The variance explained by genome-wide SNPs was achieved by fitting the GRM in a linear mixed model, via the restricted maximum likelihood method. The model is given by the following formula:

$y = \mathbf{X}\beta + \mathbf{g} + \varepsilon$

where **y** is the phenotype vector, β is a vector of fixed effects (age, sex ..), **g** is a vector of the total random genetic effects for the whole genome, and ε is a vector of residual effects.

The phenotypic variance is portioned into the variance explained by each of the genetic factors and the residual variance by the following equation:

$\mathbf{V} = \mathbf{A}\sigma^2_g + \mathbf{I}\sigma^2_\varepsilon$

where **V** is the variance of y, σ^2_g is the variance explained by all the SNPs and ***A*** is the GRM between individuals, ***I*** is an n x n identity matrix.

For shared heritability analyses, we performed a bivariate linear mixed model of two MRI phenotypes (bivariate restricted maximum likelihood analysis method).[5] The models are be given by the following equation:

$\mathbf{y}_1 = \mathbf{X}_1\mathbf{b}_1 + \mathbf{Z}_1\mathbf{g}_1 + \mathbf{e}_1$ for MRI-marker 1

$\mathbf{y}_2 = \mathbf{X}_2\mathbf{b}_2 + \mathbf{Z}_2\mathbf{g}_2 + \mathbf{e}_2$ for MRI-marker 2

where y is the phenotype vector, $\mathbf{b}_1$ and $\mathbf{b}_2$ are vectors of fixed effects, $\mathbf{g}_1$ and $\mathbf{g}_2$ are vectors of random polygenic effects, $\mathbf{e}_1$ and $\mathbf{e}_2$ are residuals for MRI phenotypes 1 and 2, **X** and **Z** are **b** and **g** incidence matrices. After determination of a variance covariance matrix, we can estimate the genetic covariance σ^2_{g1g2} and hence the genetic correlation between two MRI-markers captured by the whole genome.

For heritability and shared heritability analyses, as the 3C-Dijon cohort is a population-based study, we used the prevalence of a dichotomous trait in our cohort as an estimation of the prevalence in the population. We used the “prevalence” option available in GCTA for all dichotomous traits.

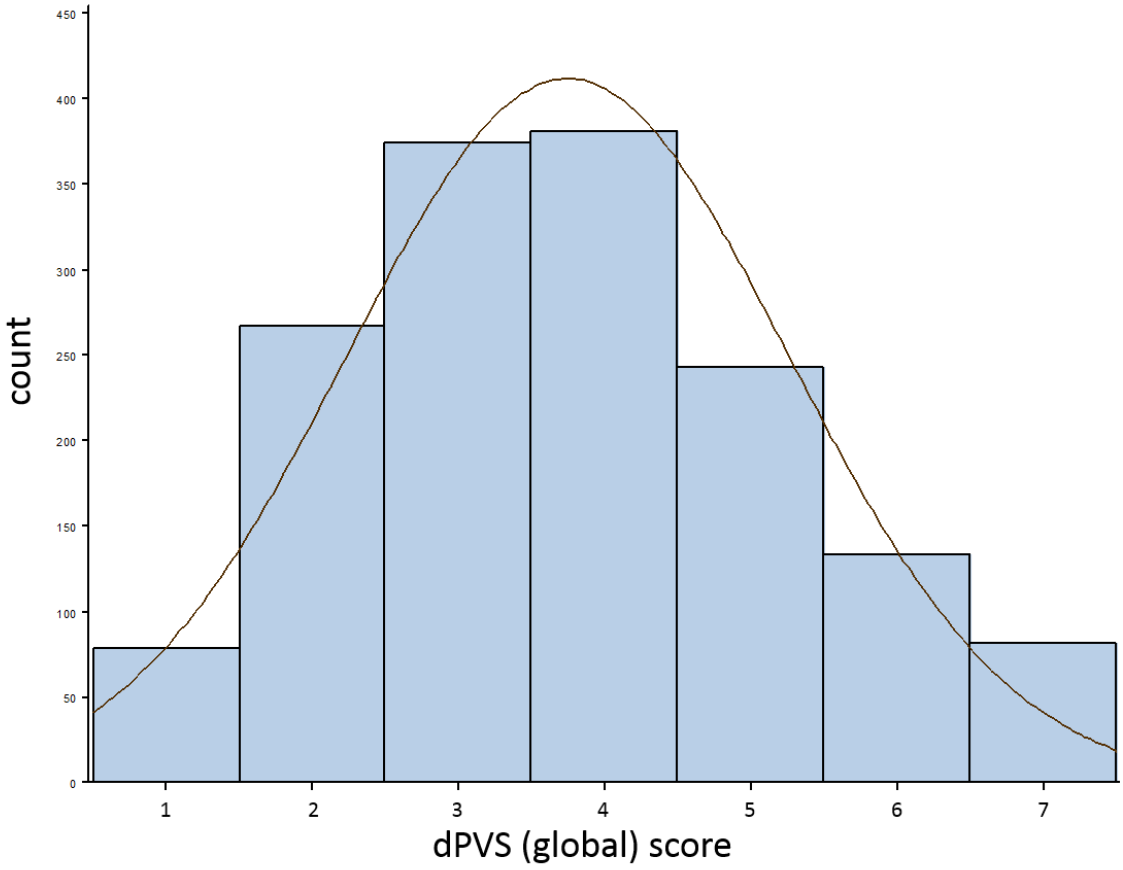

Supplementary Figure. Distribution of the dilated perivascular spaces global burden score

RESULTS

Supplementary Table I. Comparison of characteristics between included and non-included 3C-Dijon study participants under the age of 80 years at inclusion

Characteristics	Included (N=1,562)	Non-included (N=2,631)	P-Value[#]
Age at MRI in years, mean±standard deviation	72.8±4.1	NA	NA
Age at baseline in years	72.4±4.1	73.1±3.9	<0.0001
Women, N (%)	951 (60.9)	1640 (62.3)	0.430
Systolic blood pressure, mmHg	148.8±22.7	149.4 ± 22.6	0.740
Diastolic blood pressure, mmHg	84.9±11.5	84.2 ± 11.6	0.086
Pulse pressure, mmHg	63.9±17.1	65.2 ± 17.5	0.456
Hypertension status[*]	1197 (76.6)	2087 (79.4)	0.151
Type II diabetes mellitus[†]	130 (8.34)	265 (10.9)	0.008
Current smoker	95 (6.1)	134 (5.1)	0.288
History of cardiovascular disease[‡]	64 (4.1)	310 (11.8)	<0.0001
Body mass index, kg/m²	25.5±3.85	25.9±4.3	0.001
Hypercholesterolemia[§]	876 (56.2)	1538 (62.1)	0.0002
Total cholesterol, mmol/L	5.8±0.9	5.8±1.0	0.007
Low-density lipoprotein, mmol/L	3.6±0.8	3.6±0.9	0.003
Triglycerides, mmol/L	1.2±0.6	1.2±0.6	0.109
High-density lipoprotein, mmol/L	1.6±0.4	1.6±0.4	0.195
Educational level >baccalaureate[‖]	557 (35.7)	812 (30.9)	0.003

*Systolic blood pressure ≥140mmHg or diastolic blood pressure ≥90mmHg or antihypertensive drugs; [†]Blood glucose ≥7mmol/L ± antidiabetic drugs; [‡]Include myocardial infarction, arteritis, cardiac and vascular surgery (patients with stroke excluded); [§]Cholesterolemia ≥6.2mmol/L or lipid-lowering treatment; [‖]Final high-school degree in France, [#]logistic regression, between included (N=1562) and non-included participants under the age of 80 years at inclusion (N=2631), adjusted for age and sex; and for antihypertensive drug (pulse pressure, systolic and diastolic blood pressure analyses).

Supplementary Table II. Secondary analysis: heritability of dPVS in hippocampus and brain stem (top quartile)

	h^2 (SD)	P-Value	N*
dPVS (HIP)	0.52 (0.43)	0.11	1,482
dPVS (BS)	2E-6 (0.49)	0.5	1,482

Analyses were adjusted for age, sex, 20 first principal components of population stratification, and intracranial volume; *unrelated individuals up to the third degree; BS: brain stem (0-3 dPVS versus 4+); dPVS: dilated perivascular spaces; h^2: proportion of phenotypic variance explained by genome-wide SNPs; HIP: hippocampus (0-2 dPVS versus 3+); SD: standard deviation.

Supplementary Table III. Heritability of MRI-markers of cerebral small vessel disease estimated using GCTA, additionally adjusted for hypertension status

	h^2 (SD)	P-Value	N*
dPVS (global)	0.56 (0.24)	0.010	1,482
dPVS (WM)	0.80 (0.46)	0.042	1,482
dPVS (BG)	0.37 (0.65)	0.281	1,482
dPVS (HIP)	0.01 (0.39)	0.491	1,482
dPVS (BS)	0.02 (0.39)	0.479	1,482
WMHV	0.50 (0.24)	0.017	1,482
dWMHV	0.61 (0.24)	0.006	1,482
pvWMHV	0.48 (0.24)	0.019	1,482
LI	0.38 (0.81)	0.321	1,549

Analyses were adjusted for age, sex, hypertension status, 20 first principal components of population stratification; and intracranial volume (WMHV and dPVS); *unrelated individuals up to the third degree; BG: basal ganglia; BS: brainstem; dPVS: dilated perivascular spaces; dWMHV: deep WMHV; GCTA: genome-wide complex trait analysis; h^2: proportion of phenotypic variance explained by genome-wide SNPs; HIP: hippocampus; LI: lacunar brain infarcts; pvWMHV: periventricular WMHV; SD: standard deviation; WM: white matter; WMHV: white matter hyperintensity volume.

Supplementary Table IV. Heritability of MRI-markers of cerebral small vessel disease estimated using GCTA, additionally adjusted for diabetes

	h^2 (SD)	P-Value	N*
dPVS (global)	0.58 (0.24)	0.008	1,478
dPVS (WM)	0.82 (0.46)	0.037	1,478
dPVS (BG)	0.37 (0.65)	0.283	1,478
dPVS (HIP)	0.01 (0.39)	0.488	1,478
dPVS (BS)	0.03 (0.39)	0.470	1,478
WMHV	0.54 (0.24)	0.010	1,478
dWMHV	0.63 (0.24)	0.005	1,478
pvWMHV	0.52 (0.24)	0.013	1,478
LI	0.46 (0.81)	0.284	1,545

Analyses were adjusted for age, sex, diabetes, 20 first principal components of population stratification; and intracranial volume (WMHV and dPVS); *unrelated individuals up to the third degree; BG: basal ganglia; BS: brainstem; dPVS: dilated perivascular spaces; dWMHV: deep WMHV; GCTA: genome-wide complex trait analysis; h^2: proportion of phenotypic variance explained by genome-wide SNPs; HIP: hippocampus; LI: lacunar brain infarcts; pvWMHV: periventricular WMHV; SD: standard deviation; WM: white matter; WMHV: white matter hyperintensity volume.

Supplementary Table V. Association of known independent genetic risk variants for WMHV with dPVS burden

SNPs	Locus	dPVS (global)* (N=1494)		dPVS (WM)† (N=1494)		dPVS (BG)† (N=1494)	
		β (SD)	P-Value	OR (95% CI)	P-Value	OR (95% CI)	P-Value
rs7214628	17:73882148	-0.06 (0.07)	0.360	0.87 (0.7-1.07)	0.191	1.24 (0.94-1.63)	0.125
rs7894407	10:105176179	0.08 (0.06)	0.155	1.11 (0.93-1.34)	0.255	1.24 (0.96-1.6)	0.103
rs78857879	2:56135099	-0.17 (0.10)	0.088	0.97 (0.71-1.33)	0.856	0.93 (0.61-1.42)	0.732
rs2984613	1:156197380	0.03 (0.06)	0.607	1.01 (0.84-1.22)	0.916	1.12 (0.87-1.44)	0.393
rs11679640	2:43141485	0.04 (0.07)	0.616	0.90 (0.72-1.13)	0.360	1.14 (0.83-1.55)	0.419

*Linear regression; †Logistic regression; analyses were adjusted for age, sex, 4 first principal components of population stratification, and intracranial volume; BG: basal ganglia; 95% CI: 95% confidence interval; dPVS: dilated perivascular spaces; SD: standard deviation; SNPs: Single Nucleotide Polymorphisms; WM: white matter.

REFERENCES

1. Bis JC, DeCarli C, Smith AV, van der Lijn F, Crivello F, Fornage M, et al. Common variants at 12q14 and 12q24 are associated with hippocampal volume. *Nat Genet*. 2012;44:545-551
2. Verhaaren BFJ, Debette S, Bis JC, Smith JA, Ikram MK, Adams HH, et al. Multiethnic genome-wide association study of cerebral white matter hyperintensities on mri. *Circ Cardiovasc Genet*. 2015;8:398-409
3. Patterson N, Price AL, Reich D. Population structure and eigenanalysis. *PLoS Genet*. 2006;2:e190
4. Yang J, Lee SH, Goddard ME, Visscher PM. Gcta: A tool for genome-wide complex trait analysis. *The American Journal of Human Genetics*. 2011;88:76-82
5. Lee SH, Yang J, Goddard ME, Visscher PM, Wray NR. Estimation of pleiotropy between complex diseases using single-nucleotide polymorphism-derived genomic relationships and restricted maximum likelihood. *Bioinformatics*. 2012;28:2540-2542